Mechanism of One-Electron Oxidation of β-, γ-, and δ-Hydroxyalkyl Sulfides. Catalysis through Intramolecular Proton Transfer and Sulfur−Oxygen Bond Formation

Krzysztof Bobrowski,*,†,‡ Gordon L. Hug,*,‡ Bronislaw Marciniak,*,§,‡ Brian Miller,⊥ and Christian Schöneich*,⊥

Contribution from the Institute of Nuclear Chemistry and Technology, 03-195 Warsaw, Poland, Radiation Laboratory, University of Notre Dame, Notre Dame, Indiana 46556, Faculty of Chemistry, A. Mickiewicz University, 60-780 Poznan, Poland, and Department of Pharmaceutical Chemistry, University of Kansas, 2095 Constant Avenue, Lawrence, Kansas 66047

Received March 3, 1997[⊗]

Abstract: The mechanism of photoinduced electron transfer between sulfur-containing alcohols and the 4-carboxybenzophenone (CB) triplet state in aqueous solution was investigated using laser flash photolysis and steady-state photolysis techniques. Bimolecular rate constants for quenching of the CB triplet state by five hydroxyalkyl sulfides, 2-(methylthio)ethanol (2-MTE), 2,2′-dihydroxydiethyl sulfide (2,2′-DHE), 3-(methylthio)propanol (3-MTP), 3,3′-dihydroxydipropyl sulfide (3,3′-DHP), and 4-(methylthio)butanol (4-MTB), with varying numbers of OH groups and varying locations with respect to the sulfur atom, were determined to be in the range $(3.3-4.8) \times 10^9$ M^{-1} s^{-1} for neutral solutions. The intermediates identified were the CB ketyl radical anion ($CB^{\bullet-}$), the CB ketyl radical ($CBH^{\bullet}$), and intermolecularly (S∴S)-bonded radical cations. An additional absorption band at approximately 400 nm in the transient spectra for some of the hydroxyalkyl sulfides was assigned to the intramolecularly ($^{\bullet}$S−O)-bonded species (only for hydroxyalkyl sulfides which could adopt a five-membered ring structure). The spectra of appropriate $(S\therefore S)^+$ and ($^{\bullet}$S−O) intermediates for the hydroxyalkyl sulfides were determined from complementary pulse radiolysis studies in acid and neutral aqueous solutions of the hydroxyalkyl sulfides, respectively. The observation of ketyl radical anions and intermolecular (S∴S)-bonded radical cations of the hydroxyalkyl sulfides was direct evidence for the participation of electron transfer in the mechanism of quenching. Quantum yields of formation of intermediates from flash photolysis experiments and quantum yields of formaldehyde formation from the steady-state measurements were determined. The values of these quantum yields indicated that the diffusion apart (escape of the radical ions) of the charge-transfer complex, formed as a primary photochemical step, is a minor photochemical pathway (with a contribution of ∼5−25% depending on the numbers of OH groups). Competing processes of proton transfer and back electron transfer within the CT complex gave significant contributions to these yields. Detailed mechanisms for the CB-sensitized photooxidation of sulfur-containing alcohols are proposed, discussed, and compared with that for the $^{\bullet}$OH-induced oxidation. One striking feature of the mechanisms is that there is a catalytic influence of neighboring groups on the radical reaction pathways during one-electron oxidation of the hydroxyalkyl sulfides in comparison to comparable reactions of nonsubstituted alkyl sulfides. Support for the mechanisms came in part from an analysis of observed solvent isotope effects on radical quantum yields.

Introduction

Organic sulfides play an important role as structural elements in many materials and biological macromolecules. Because of their high susceptibility to oxidation any attempt to maintain the integrity of such sulfides requires a detailed understanding of the underlying mechanisms as well as the physico-chemical parameters which control oxidation reactions. A field which would particularly benefit from such knowledge is the biotechnological production of recombinant proteins where methionine residues often suffer oxidation during processing, purification, and storage.[1]

In proteins, methionine residues are potentially surrounded by a variety of neighboring groups such as carboxylate, amino, hydroxy, and amide functionalities most of which have been shown to affect sulfide oxidations in simple organic model compounds.[2−5] The attacking oxidant usually induces formation of a distinct intermediate at the sulfide site, and the nature of this intermediate circumscribes the scope of any subsequent participation of neighboring groups. The nature and strength of the coupling of the neighboring group to any attacking oxidizing species and/or to the intermediate moiety formed at the sulfide site affects the ultimate course of the sulfide oxidation. Reactions that start as simple one-electron oxidations can, through interactions with neighboring groups, end up as transient species that are susceptible to carbon−carbon bond fragmentation.

An illustration of how these themes play out can be seen in the oxidation of the dipeptide threonylmethionine (Thr-Met) by two different one-electron oxidants, the hydroxyl radical, $^{\bullet}$OH, and the sulfate radical anion $SO_4^{\bullet-}$.[6] The reaction with $^{\bullet}$OH

† Institute of Nuclear Chemistry and Technology.
‡ University of Notre Dame.
§ A. Mickiewicz University.
⊥ University of Kansas.
⊗ Abstract published in *Advance ACS Abstracts,* August 15, 1997.

(1) Manning, M. C.; Patel, K.; Borchardt, R. T. *Pharm. Res.* **1989**, *6*, 903−918.
(2) Glass, R. S.; Hojjatie, M.; Wilson, G. S.; Mahling, S.; Göbl, M.; Asmus, K.-D. *J. Am. Chem. Soc.* **1984**, *106*, 5382−5383.
(3) Asmus, K.-D.; Göbl, M.; Hiller, K.-O.; Mahling, S.; Mönig, J. *J. Chem. Soc., Perkin Trans. 2* **1985**, 641−646.
(4) Mahling, S.; Asmus, K.-D.; Glass, R. S.; Hojjatie, M.; Wilson, G. S. *J. Org. Chem.* **1987**, *52*, 3717−3724.
(5) Steffen, L. K.; Glass, R. S.; Sabahi, M.; Wilson, G. S.; Schöneich, C.; Mahling, S.; Asmus, K.-D. *J. Am. Chem. Soc.* **1991**, *113*, 2141−2145.

S0002-7863(97)00683-5 CCC: $14.00

leads to a sequence of reactions: (i) formation of a hydroxysulfuranyl radical, $>^{\bullet}S-OH$, (ii) coupled proton/electron transfer from the N-terminal amino group to the hydroxysulfuranyl radical, and (iii) formation of a nitrogen-centered radical cation which induces a carbon−carbon fragmentation of the Thr side chain. In contrast, the oxidation by $SO_4^{\bullet-}$ results in the formation of a relatively stable cyclic S−O bond that is formed through interaction of an initially formed sulfur radical cation $>S^{\bullet+}$ with the C-terminal carboxylate group. The difference between these two one-electron oxidation pathways appears to originate from the initial interaction of the two oxidizing species with the sulfur, i.e., hydroxysulfuranyl radical vs sulfur radical cation. Subsequently these initially formed intermediates at the sulfide site interact with different neighboring groups, i.e., N-terminal amino group vs C-terminal carboxylate group. Other examples for such mechanisms exist, i.e., the oxidation of γ-glutamylmethionine and analogs by $^{\bullet}OH$,[7−9] $SO_4^{\bullet-}$,[10] and *S*-alkylglutathiones by $^{\bullet}OH$[11] and triplet 4-carboxybenzophenone.[12]

Hydroxyalkyl sulfides provide conceptually simpler models for understanding neighboring-group participation in the oxidation of the sulfides than threonylmethionine. However, even with these compounds complications arise. For instance, when $^{\bullet}OH$ radicals reacted with 2-(methylthio)ethanol (2-MTE) and 2,2′-dihydroxydiethyl sulfide (2,2′-DHE),[13] an initially formed hydroxysulfuranyl radical immediately fragmented to yield alkylthiomethyl radicals and formaldehyde (reaction 1).

$$RS^{\bullet}(OH)CH_2CH_2OH \rightarrow {}^{\bullet}CH_2SR + H_2O + CH_2{=}O \quad (1)$$

No intermediary sulfur radical cations were observed at neutral to alkaline pH. On the other hand, when sulfur radical cations or their dimeric three-electron bonded complexes were generated at low pH (reaction 2),

$$^{\bullet}OH + 2RSCH_2CH_2OH + H^+ \rightarrow [(R)(HOCH_2CH_2)S\therefore S(CH_2CH_2OH)(R)]^+ + H_2O \quad (2)$$

they were quite stable toward fragmentation, as will be shown in this paper. The dimeric complex, symbolized as $(S\therefore S)^+$, exists in equilibrium 3 with its monomeric form.

$$(S\therefore S)^+ \rightleftarrows RSCH_2CH_2OH + R(S^{\bullet+})CH_2CH_2OH \quad (3)$$

In general, these β-hydroxy substituted radical cations, such as $R(S^{\bullet+})CH_2CH_2OH$ in equilibrium 3, are expected to undergo fragmentation of the carbon−carbon bond subsequent to base-catalyzed deprotonation of the β-hydroxy group. As evidence for this, Lucia et al.[14] reported a solvent kinetic isotope effect of $k_H/k_D = 2.0$ for the pyridine-catalyzed fragmentation of radical cations from 2-(*N*-phenylamino)-1,2-diphenylethanol, and Baciocchi et al.[15] obtained $k_H/k_D = 1.2-1.4$ for the hydroxide/water-catalyzed fragmentation of arylalkanol radical cations. However, no solvent isotope effect was observed for the decomposition of hydroxysulfuranyl radicals of 2-MTE and 2,2′-DHE.[13] For this reason, it was suggested that the mechanism of this reaction did not involve intermediary radical cations. Instead it was proposed that the mechanism involved a hydrogen transfer between the β-hydroxy group and the oxygen of the hydroxysulfuranyl moiety via a cyclic transition state (left-hand side of reaction 4) to yield an alkoxy radical (reaction 4).

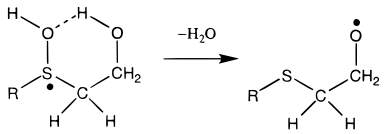

(4)

The latter, $RS(CH_2)_2O^{\bullet}$, would subsequently suffer fragmentation of the carbon−carbon bond (reaction 5).

$$RS(CH_2)_2O^{\bullet} \rightarrow {}^{\bullet}CH_2SR + CH_2{=}O \quad (5)$$

However, it was found[13] that the hydroxyl radical-induced fragmentation only yielded 40−50% formaldehyde, but α-(alkylthio)alkyl radicals, $^{\bullet}CH_2SR$, were produced quantitatively. The inequality in the yields of α-(alkylthio)alkyl radicals and formaldehyde can be accounted for by an intramolecular hydrogen transfer from the $C_\alpha-H$ bond of the substituent R in the alkoxyl radical $RS(CH_2)_2O^{\bullet}$.

$$RS(CH_2)_2O^{\bullet} \rightarrow R'C^{\bullet}HSCH_2CH_2OH \quad (6)$$

This reaction is in competition with the $C_\alpha-C_\beta$ fragmentation of $RS(CH_2)_2O^{\bullet}$ (reaction 5), and it resolves the discrepancy in yields because it produces α-(alkylthio)alkyl radicals but no formaldehyde. In reaction 6, $R- = R'CH_2-$.

The present paper investigates (i) the general mechanism of one-electron oxidation of hydroxy-substituted aliphatic sulfides, (ii) the neighboring-group participation on the formation of radical cationic intermediates, and (iii) the mechanism of carbon−carbon bond fragmentation subsequent to one-electron oxidation of 2-(methylthio)ethanol and 2,2′-dihydroxydiethyl sulfide. This paper provides further evidence that indeed typical one-electron oxidants such as triplet 4-carboxybenzophenone (CB) react via a different mechanism than hydroxyl radicals. The key step during the triplet 4-carboxybenzophenone-induced oxidation is the initial formation of a charge-transfer complex, as now shown for various substituted thioethers.[16−22] Within this charge-transfer complex formed from the CB triplet and the hydroxy-substituted alkyl sulfides, it will be shown that one reaction involves proton-transfer from the γ-hydroxy-substituted

(6) Schöneich, C.; Zhao, F.; Madden, K. P.; Bobrowski, K. *J. Am. Chem. Soc.* **1994**, *116*, 4641−4652.
(7) Bobrowski, K.; Schöneich, C.; Holcman, J.; Asmus, K.-D. *J. Chem. Soc., Perkin Trans. 2* **1991**, 353−362.
(8) Bobrowski, K.; Schöneich, C.; Holcman, J.; Asmus, K.-D. *J. Chem. Soc., Perkin Trans. 2* **1991**, 975−980.
(9) Bobrowski, K.; Schöneich, C. *Radiat. Phys. Chem.* **1996**, *47*, 507−510.
(10) Bobrowski, K.; Schöneich, C. Unpublished results.
(11) Bobrowski, K.; Pogocki, D.; Hug, G. L.; Schöneich, C. **1997**, manuscript in preparation.
(12) Bobrowski, K.; Hug, G. L.; Marciniak, B. Unpublished results.
(13) Schöneich, C.; Bobrowski, K. *J. Am. Chem. Soc.* **1993**, *115*, 6538−6547.
(14) Lucia, L. A.; Burton, R. D.; Schanze, K. S. *J. Phys. Chem.* **1993**, *97*, 9078−9080.
(15) Baciocchi, E.; Bietti, M.; Putignani, L.; Steenken, S. *J. Am. Chem. Soc.* **1996**, *118*, 5952−5960.
(16) Guttenplan, J. B.; Cohen, S. G. *J. Org. Chem.* **1973**, *38*, 2001−2007.
(17) Bobrowski, K.; Marciniak, B.; Hug, G. L. *J. Photochem. Photobiol., A* **1994**, *81*, 159−168.
(18) Marciniak, B.; Bobrowski, K.; Hug, G. L.; Rozwadowski, J. *J. Phys. Chem.* **1994**, *98*, 4854−4860.
(19) Bobrowski, K.; Marciniak, B.; Hug, G. L. *J. Am. Chem. Soc.* **1992**, *114*, 10279−10288.
(20) Marciniak, B.; Bobrowski, K.; Hug, G. L. *J. Phys. Chem.* **1993**, *97*, 11937−11943.
(21) Bobrowski, K.; Hug, G. L.; Marciniak, B.; Kozubek, H. *J. Phys. Chem.* **1994**, *98*, 537−544.
(22) Marciniak, B.; Hug, G. L.; Bobrowski, K.; Kozubek, H. *J. Phys. Chem.* **1995**, *99*, 13560−13568.

Table 1. Rate Constants for Quenching of the CB-Triplet by the Sulfur-Containing Alcohols in Aqueous Solution at pH = 6.8 (Phosphate Buffer)

alcohol	formula	abbreviation	$k_q \times 10^{-9}$ [a] (M^{-1} s^{-1})
2-(methylthio)ethanol	$H_3CSCH_2CH_2OH$	2-MTE	4.8 ± 0.1
2,2′-dihydroxydiethyl sulfide	$HOCH_2CH_2SCH_2CH_2OH$	2,2′-DHE	3.3 ± 0.1
3-(methylthio)propanol	$H_3CSCH_2CH_2CH_2OH$	3-MTP	4.4 ± 0.2
3,3′-dihydroxydipropyl sulfide	$HOCH_2CH_2CH_2SCH_2CH_2CH_2OH$	3,3′-DHP	3.6 ± 0.2
4-(methylthio)butanol	$H_3CSCH_2CH_2CH_2CH_2OH$	4-MTB	4.2 ± 0.1

[a] Errors are twice the standard deviations from the least-squares fits.

sulfides which catalyzes the oxidation under formation of intramolecular sulfur−oxygen bonds.

Experimental Details

Materials. 4-Carboxybenzophenone (CB) and the hydroxyalkyl sulfides, 2-(methylthio)ethanol (2-MTE), 2,2′-dihydroxydiethyl sulfide (2,2′-DHE), 3-(methylthio)propanol (3-MTP), 3,3′-dihydroxydipropyl sulfide (3,3′-DHP), and 4-(methylthio)butanol (4-MTB), obtained from Aldrich Chemical Company, were of the purest commercially available grade and were used as received. (2,4-Dinitrophenyl)hydrazine was from Eastman Chemicals. Formaldehyde was purchased from Fisher Chemical (Fair Lawn, NJ) as a 37% (w/w) aqueous solution. HPLC grade acetonitrile was supplied by Fisher Chemical (Fair Lawn, NJ). Water was purified by a Millipore Milli-Q system. Deuterium oxide (D_2O) was supplied by DOE, Savannah River State.

Laser Flash Photolysis Experiments. The nanosecond laser flash photolysis setup has been described generaly elsewhere[23,24] and also as specifically configured in this work.[25] The concentration of CB was 2×10^{-3} M in all experiments. The concentrations of alcohols were in the range 2×10^{-5}−2×10^{-4} M in the quenching experiments, but the concentrations of these quenchers were 0.02 M for the quantum yield determinations and for the experiments that involved recording transient spectra in the time range following complete quenching (>99.5%) of the CB triplet state. Transient absorption spectra and quantum yield measurements were performed using a flow-cell system. Typically five to seven laser shots were averaged for each kinetic trace. The pH of the solutions was adjusted by adding sodium hydroxide and/or $HClO_4$. All solutions were deoxygenated by bubbling high-purity argon through them.

Pulse Radiolysis Experiments. Pulse radiolysis experiments were performed with 10 ns pulses of high-energy electrons from the Notre Dame 7 MeV ARCO LP-7 linear accelerator and the Notre Dame Titan Beta Model TBS-8/16−1S electron linear accelerator. Absorbed doses were on the order of 4−6 Gy (1 Gy = 1 J/kg). N_2O-saturated 10^{-2} M solutions of potassium thiocyanate were used as the dosimeter, taking a radiation chemical yield of 6.13 and a molar extinction coefficient of 7580 M^{-1} cm^{-1}. A description of the pulse radiolysis setup, data collection system, and details of dosimetry has been reported elsewhere.[26,27] The data acquisition subsystem has been updated[28] and includes a Spex 270M monochromator, a LeCroy 7200A transient digitizer, and a PC-AT compatible computer. The software was written within LabWindows of National Instruments.[28] The experiments were carried out with continuously flowing solutions.

Steady-State Photolysis Experiments. The irradiations were performed in quartz cells with a Rayonet photoreactor equipped with 300 nm lamps. A solution of ferrioxalate was used as an actinometer,[29] and the intensity of the incident light was determined to be 6.29×10^{-6} einstein dm^{-3} s^{-1}. Solutions containing CB (5×10^{-4} M) and a hydroxyalkyl sulfide (6×10^{-3} M) at appropriate pH's were purged with oxygen-free nitrogen, passed through an OxiClear disposable gas purifier (LabClear, Oakland, CA), and irradiated. The consumption of CB and the formation of pinacol were determined by means of HPLC, employing an SGE polymer-coated C18 column (4 × 250 mm), an isocratic mobile phase consisting of 40% (v/v) acetonitrile and 0.1% (v/v) trifluoroacetic acid, and UV detection at 254 nm. The quantum yields of formaldehyde were determined by dividing the absolute yields of formaldehyde by the initial yields of the CB triplet state. The yields of the CB triplet state were deduced from the pinacol yields obtained during photoirradiation of N_2-saturated aqueous solutions containing 0.1 M 2-propanol in water and 2×10^{-2} M phosphate buffer, pH 7.0. The quantum yields were calculated on the basis that each CB triplet should yield 0.93 equiv of pinacol and lead to the consumption of 1.86 equiv of the CB ground state.

The time of irradiation was chosen so that <10% CB conversion occurred during the formation of $H_2C{=}O$.

HPLC Analysis of Formaldehyde. The analysis of formaldehyde was carried out by derivatization with (2,4-dinitrophenyl)hydrazine followed by HPLC analysis according to two different procedures. A 1-mL aliquot of an irradiated solution was reacted for 10 min with 1 mL of a solution of 10^{-2} M (2,4-dinitrophenyl)hydrazine in 10^{-2} M HCl. Subsequently the reaction mixture was extracted with 1 mL of an *n*-hexane/CH_2Cl_2 (80:20, v/v) mixture by stirring for 5 min. The HPLC analysis was performed employing a Shimadzu HPLC, equipped with a UV detector. The organic layer, containing the hydrazone, was separated from the aqueous phase, and a 5 μL aliquot was injected into an HPLC column (SGE Hypersil C18, 5 micron, 250 × 4.6 mm) which was eluted isocratically with acetonitrile/water, 60:40 (v/v), at a flow rate of 1 mL/min. The hydrazones were monitored by UV detection at 345 nm. Under the HPLC conditions the formaldehyde hydrazone eluted with $t_R = 3.9$ min. In a second procedure, 20 μL of the reaction mixture were directly (without extraction) injected into a Varian RPC 18 column (5 micron, 4.6 × 150 mm) which was eluted isocratically with a mobile phase consisting of 40:60 acetonitrile/water (v/v), containing 0.1% trifluoroacetic acid. Under these conditions the retention time of the formaldehyde hydrazone was 9.5 min. Both methods gave identical results. Calibration was achieved by conducting the same procedure with authentic formaldehyde samples.

Results

Rate Constants of Quenching the CB Triplet State by Hydroxyalkyl Sulfides. Five hydroxyalkyl sulfides (Table 1) were used as quenchers of the CB triplet state in aqueous solution at pH 6.8 (phosphate buffer). The CB triplet state is always in its carboxylate form at pH > 6.3 ($pK_a = 4.5$ for CB), and the hydroxyalkyl sulfides are in their nonionic form at neutral and alkaline pH.

The triplet quenching rate constants k_q were measured by monitoring the triplet−triplet (T−T) absorption decays (k_{obs}) of CB at wavelengths of 420, 480, and 540 nm. The latter corresponds to the spectral maximum of the CB triplet, but interference by the growth of absorbing electron-transfer intermediates made the other wavelengths more favorable for monitoring triplet decays in most instances.

The pseudo-first-order rate constants, k_{obs}, were calculated using eq I which takes into account a concomitant, underlying first-order growth of a photoproduct's absorption[30]

(23) Encinas, M. V.; Scaiano, J. C. *J. Am. Chem. Soc.* **1979**, *101*, 2146−2152.
(24) Nagarajan, V.; Fessenden, R. W. *J. Phys. Chem.* **1985**, *89*, 2330−2335.
(25) Hug, G. L.; Marciniak, B.; Bobrowski, K. *J. Phys. Chem.* **1996**, *100*, 14914−14921.
(26) Janata, E.; Schuler, R. H. *J. Phys. Chem.* **1982**, *86*, 2078−2084.
(27) Schuler, R. H. *Chem. Educ.* **1985**, *2*, 34−37.
(28) Wang, Y. **1993**, Unpublished report.
(29) Murov, S. L.; Carmichael, I.; Hug, G. L. *Handbook of Photochemistry*, 2nd ed.; Dekker: New York, 1993.
(30) Encinas, M. V.; Wagner, P. J.; Scaiano, J. C. *J. Am. Chem. Soc.* **1980**, *102*, 1357−1360.

$$\ln\left(\frac{A - A_\infty}{A_0 - A_\infty}\right) = -k_{obs}t \qquad \text{(I)}$$

where A_0, A, A_∞ are the absorbance changes at time 0, t, and infinity, respectively.

The quenching rate constants, k_q, were determined from a linear least-squares fit of k_{obs} vs [Q] plots employing the pseudo-first-order relation

$$k_{obs} = (\tau_T)^{-1} + k_q[Q] \qquad \text{(II)}$$

where τ_T is the lifetime of the CB triplet in the absence of quencher. The resulting quenching rate constants obtained for all the hydroxyalkyl sulfides are listed in Table 1 along with the estimated uncertainties in the measurements.

Pulse Radiolysis. Pulse radiolysis experiments were performed in order to obtain spectra of the isolated dimeric radical cations $(S\therefore S)^+$ and the various radicals with sulfur−oxygen bonds. Experiments were done with each of the appropriate hydroxyalkyl sulfides. Both types of sulfur-centered radicals are possible electron-transfer products from the quenching reactions of the CB triplet with the various hydroxyalkyl sulfides. The spectra of these radicals were then used as possible components in the analysis of the transient spectra following the triplet-quenching events (vide infra).

$(S\therefore S)^+$ dimeric radical cations were generated in N_2-saturated solutions with high concentrations, 0.01−0.1 M, of the hydroxyalkyl sulfides at pH 1. A solution of low pH (acidified with perchloric acid) was used to ensure a high concentration of the protons to promote the elimination of water[3,31] according to reaction 7.

$$>^{\bullet}S{-}OH + H^+ \rightarrow >S^{\bullet+} + H_2O \qquad (7)$$

These conditions were employed in order to severely limit competing reactions of the initial hydroxysulfuranyl radicals $>^{\bullet}S{-}OH$ which can lead to other transients.[13] In particular, the excess protons would favor reaction 7 over reaction 4 followed by reactions 5 and 6 (for 2-MTE and 2,2′-DHE). Likewise, reaction 7 would be favored over reaction 8 (for 3-MTP and 3,3′-DHP).

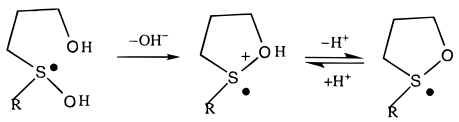

(8)

In the following, the type of radical in the middle structure of reaction 8 will be referred to as $(^{\bullet}S{-}OH)^+$, whereas the deprotonated type on the far right-hand side of reaction 8 will be referred to as $(^{\bullet}S{-}O)$. (In model systems, the S−O bond in the protonated radical species appears to be closer to being hydroxysulfuranyl in nature as opposed to a two-center three-electron bond.[32])

High concentrations of the hydroxyalkyl sulfides facilitated the formation of dimer radical cations through reaction of a $>S^{\bullet+}$ radical with a nonoxidized hydroxyalkyl sulfide (reaction 9)

$$>S^{\bullet+} + S< \rightleftarrows (>S\therefore S<)^+ \qquad (9)$$

and through the water-assisted reaction[13] of the hydroxysulfuranyl radical ($>^{\bullet}S{-}OH$) with a nonoxidized hydroxyalkyl sulfide (reaction 10).

$$>^{\bullet}S{-}OH + S< \rightleftarrows (>S\therefore S<)^+ + OH^- \qquad (10)$$

The yields of $(S\therefore S)^+$ dimeric radical cations were assumed to be equal to the yields of the primary $>^{\bullet}S{-}OH$ adducts where these yields are equal to 80% of the total available $^{\bullet}OH$ radicals (G_{total} = 3.0 radicals per 100 eV absorbed).[3,33] The molar absorption coefficients reported in Table 2 are based on 10 separate determinations at the spectral maxima in question and are based on $G_{80\%}$ = 2.4 radicals per 100 eV of energy absorbed in N_2-saturated solutions of the hydroxyalkyl sulfides at pH 1. They compare well with the ϵ's (4000−9000 M^{-1} cm^{-1}) of other $(R_2S\therefore SR_2)^+$ radical cations.[4,31,33−37] Only for 3,3′-DHP was the molar absorption coefficient corrected for contributions from the $(^{\bullet}S{-}OH)^+$ transient (vide infra).

The spectra of $(^{\bullet}S{-}O)$ transients were obtained from N_2O-saturated aqueous solutions of 3-MTP and 3,3′-DHP (1×10^{-4} M) at pH 6.8. The higher pH and relatively low concentrations of the hydroxyalkyl sulfides were used to avoid competitive production of $(S\therefore S)^+$ radical cations that might be formed in competition with the intramolecularly bonded $(^{\bullet}S{-}O)$ radicals,[4] as shown in reaction 8. Under these experimental conditions, the radiation chemical yield of the hydroxyl radicals, available for reaction with the thioethers, was $G(^{\bullet}OH)$ = 5.3 (based on the formula given by Schuler et al.[38] which relates the G-value of solute radicals generated by $^{\bullet}OH$ radicals to the product of the rate constant for the reaction of $^{\bullet}OH$ with the solute and the solute concentration). Assuming the yield of intramolecularly sulfur−oxygen bonded radicals to be equal to the yield of the $>^{\bullet}S{-}OH$ adduct (= $G_{80\%}$), $G \approx 4.25$ can be estimated. Molar absorption coefficients based on this yield are reported in Table 2.

As reported previously,[4,39] the oxidation of the alcohols containing the thioether functionality leads to a radical species which exists in acid−base equilibrium, as shown in reaction 8. The acidic forms of the $(^{\bullet}S{-}O)$ radicals formed from 3-MTP and 3,3′-DHP absorb at λ_{max} = 390 nm with ϵ's of ≈1000 and 1450 M^{-1} cm^{-1}. Their basic forms absorb at λ_{max} = 400 nm with ϵ = 3250 and 2700 M^{-1} cm^{-1}, respectively. For the present discussion it is noteworthy that the acidity of the hydroxyl group in the radicals with sulfur−oxygen bonds is greatly enhanced over that of the unoxidized hydroxyalkyl sulfides (see Discussion).

Transient Absorption Spectra of Intermediates during Photolysis. Aqueous solutions of 4-carboxybenzophenone and the various hydroxyalkyl sulfides that were used in the flash photolysis and steady-state photolysis experiments were first examined spectroscopically for any evidence of ground-state association. The absorption spectra of these mixtures were shown to be equal to those expected by adding the spectra from separate solutions of ketone and quencher. No evidence for ground-state association was found under the experimental conditions used.

The fate of the reactions after the laser flash were followed by analyzing the optical absorption spectra of the transients. A flow system was used, and individual kinetic traces were

(31) Bonifacic, M.; Möckel, H.; Bahnemann, D.; Asmus, K.-D. *J. Chem. Soc., Perkin Trans. 2* **1975**, 675−685.
(32) Carmichael, I. **1997**, private communication.
(33) Hiller, K.-O.; Masloch, B.; Göbl, M.; Asmus, K.-D. *J. Am. Chem. Soc.* **1981**, *103*, 2734−2743.
(34) Göbl, M.; Bonifacic, M.; Asmus, K.-D. *J. Am. Chem. Soc.* **1984**, *106*, 5984−5988.
(35) Mohan, H.; Mittal, J. P. *Radiat. Phys. Chem.* **1991**, *38*, 45−50.
(36) Mohan, H.; Mittal, J. P. *J. Chem. Soc., Perkin Trans. 2* **1992**, 207−212.
(37) Chaudhri, S. A.; Mohan, H.; Anklam, E.; Asmus, K.-D. *J. Chem. Soc., Perkin Trans. 2* **1996**, 383−390.
(38) Schuler, R. H.; Hartzell, A. L.; Behar, B. *J. Phys. Chem.* **1981**, *85*, 192−199.
(39) Glass, R. S.; Hojjatie, M.; Petsom, A.; Wilson, G. S.; Göbl, M.; Mahling, S.; Asmus, K.-D. *Phosphorus Sulfur* **1985**, *23*, 143−168.

Table 2. Spectral Data of Intermolecular $(S\therefore S)^+$ Type Dimeric Radical Cations and Intramolecular ($^\bullet$S−O) Type Radicals for the Sulfur-Containing Alcohols in Aqueous Solutions Obtained by the Pulse Radiolysis Technique

	$(S\therefore S)^+$ [a]		($^\bullet$S−O)[d]	
alcohol	λ_{max} (nm)	ϵ (M^{-1} cm^{-1})	λ_{max} (nm)	ϵ (M^{-1} cm^{-1})
2-MTE	475	8100[b]	*e*	*e*
2,2′-DHE	500	8100[b]	*e*	*e*
3-MTP	480	8400[b]	400	3250[f]
3,3′-DHP	500	7300[c]	400	2700[f]
4-MTB	480	8250[b]	*g*	*g*

[a] [2-MTE, 3-MTP, 3,3′-DHP, 4-MTB] = 0.01 M; [2,2′-DHE] = 0.1 M, pH = 1, N_2-saturated. [b] Taking $G(S\therefore S)^+ = 2.4$ which is 80% of the available $^\bullet$OH radicals, total $G(^\bullet OH) = 3.0$, standard deviation of measurements ±10%. [c] Calculated value taking $G(^\bullet OH) = 2.4$ (80% of the available $^\bullet$OH radicals) as the sum of $(S\therefore S)^+$ and ($^\bullet$S−O) formation and assuming that the spectra of $(S\therefore S)^+$ for 3,3′-DHP and 2,2′-DHE have the same shape (see text). [d] [3-MTP, 3,3′-DHP] = 10^{-4} M, pH 6.8, N_2O-saturated. [e] Cannot form stable cyclic ($^\bullet$S−O)-bonded intermediates. [f] Taking $G(^\bullet S{-}O) = 4.25$ which is 80% of the available $^\bullet$OH radicals, total $G(^\bullet OH) = 5.3$; standard deviation of measurements ±10%. [g] Does not form stable ($^\bullet$S−O)-bonded intermediates (see text).

collected at 10 nm intervals. Time-resolved spectra were generated from these sets of traces, choosing appropriate time delays and appropriate time windows. Spectra, so generated, were resolved into component transients by a linear regression technique[40] of the form

$$\Delta A(\lambda_j) = \sum_{i=1}^{n} \epsilon_i(\lambda_j)\alpha_i \qquad \text{(III)}$$

where $\Delta A(\lambda_j)$ is the observed absorbance change of the composite spectrum and $\epsilon_i(\lambda_j)$ is the molar absorption coefficient of the *i*th species at the *j*th wavelength of observation. The linear regression coefficients, a_i, correspond to $c_i l$ (where c_i is the concentration of the *i*th transient and *l* is the optical pathlength of the monitoring light). Further details of this method have been described elsewhere.[20] The spectra of the CB triplet, CB ketyl radicals CBH$^\bullet$, and CB ketyl radical anions CB$^{\bullet-}$ were taken from previous work[22,41] with renormalized values of the molar absorption coefficients (ϵ_{535} = 6250 M^{-1} cm^{-1}, ϵ_{570} = 5200 M^{-1} cm^{-1}, and ϵ_{660} = 7660 M^{-1} cm^{-1} for ^{3}CB*, CBH$^\bullet$, and CB$^{\bullet-}$, respectively).[42,43] The component spectra $\{\epsilon_i(\lambda_j)\}$ of the transients from the hydroxyalkyl sulfides were generated by pulse radiolysis (as mentioned above) for this work.

Flash excitation of a solution of 4-carboxybenzophenone (2×10^{-3} M) and the various hydroxyalkyl sulfides (0.02 M) resulted in the appearance of the absorption corresponding to various transients depending on the time delay, the structure of the hydroxyalkyl sulfide used, and the pH of the solution. High concentrations of the hydroxyalkyl sulfides were used to rapidly quench more than 99% of the CB triplets.

When the CB triplet was quenched by the hydroxyalkyl sulfides, the resulting transient absorption spectra had spectral features reminiscent of the CB-triplet, the ketyl radical anion, and the ketyl radical. A typical transient absorption spectrum of this type, obtained for 2-MTE at pH 6.9, is presented in Figure 1. The transient at 570 nm is associated with the ketyl radical

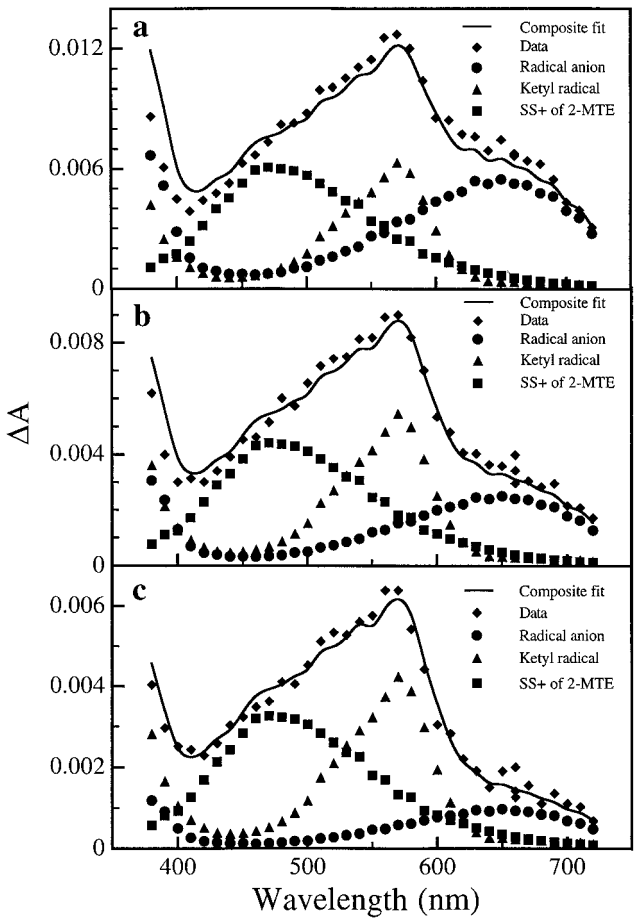

Figure 1. Resolution of the spectral components in the transient absorption spectra following the quenching of CB-triplet by 2-MTE (0.02 M) at pH 6.9 (without buffer) taken (a) 1.2 μs, (b) 14.1 μs and (c) 31.6 μs after the flash.

(CBH$^\bullet$) of CB, and that at 480 nm is assigned to the intermolecularly S∴S-bonded radical cation.

Spectra taken near pH 10 show a transient absorbing at 660 nm which is assigned to the ketyl radical anion (CB$^{\bullet-}$). For the quenching of ^{3}CB* by the hydroxyalkyl sulfides 3-MTP and 3,3′-DHP, one additional intermediate could be identified from the composite spectra. As shown in Figure 2, the presence of an intermediate absorbing in the short-wavelength region around 400 nm is required to get a reasonably good composite fit with the experimental data at pH 6.8 for 3-MTP.

That intermediate is suggested to be an intramolecularly ($^\bullet$S−O)-bonded species (see species on the far right of reaction 8). Formation of this intermediate requires interaction of the unpaired electron of the sulfur with a free electron pair of the oxygen atom of the hydroxyl group. Its formation is assisted by a suitable conformational arrangement (five-membered ring).

Intramolecular ($^\bullet$S−O)-bonded radicals derived from 3-MTP and 3,3′-DHP (see structures in reaction 8) were characterized in the Pulse Radiolysis section above. The presence of intramolecular ($^\bullet$S−O)-bonded radicals was previously confirmed in pulse radiolysis[2−5,44,45] and laser flash photolysis[18] experiments with sulfur-containing acids and amino acids. At pH = 9.8 resolutions of the experimental transient absorption spectra also led to the presence of the intermolecular S∴S-bonded radical cations and the intramolecular ($^\bullet$S−O)-bonded radicals, but at this pH both species had much shorter lifetimes than did the corresponding species at lower pH.

(40) Bevington, P. R. *Data Reduction and Error Analysis for the Physical Sciences*; McGraw-Hill: New York, 1969.
(41) Inbar, S.; Linschitz, H.; Cohen, S. G. *J. Am. Chem. Soc.* **1981**, *103*, 7323−7328.
(42) Hurley, J. K.; Sinai, N.; Linschitz, H. *Photochem. Photobiol.* **1983**, *38*, 9−14.
(43) Hurley, J. K.; Linschitz, H.; Treinin, A. *J. Phys. Chem.* **1988**, *92*, 5151−5159.
(44) Mohan, H. *J. Chem. Soc., Perkin Trans. 2* **1990**, 1821−1824.
(45) Bobrowski, K.; Holcman, J. *J. Phys. Chem.* **1989**, *93*, 6381−6387.

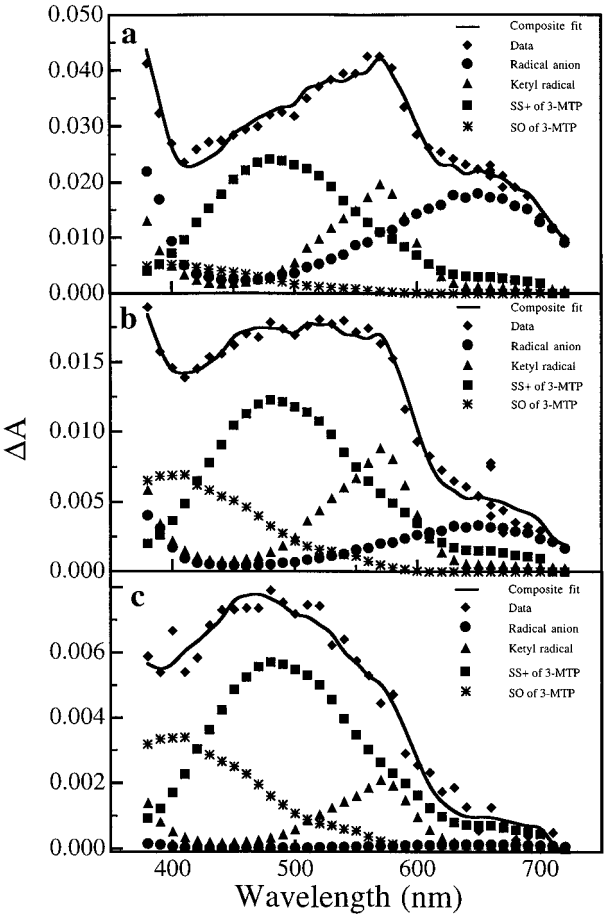

Figure 2. Resolution of the spectral components in the transient absorption spectra following the quenching of CB-triplet by 3-MTP (0.02 M) at pH 6.8 (without buffer) taken (a) 780 ns, (b) 11.7 μs, and (c) 31.2 μs after the flash.

In the case of the hydroxyalkyl sulfide 4-MTB, the composite transient spectra at pH 6.1 and 10.0 (Figure 3) can be resolved into a contribution from the intermolecularly (S∴S)-bonded radical cation ($\lambda_{max} = 480$ nm) along with a contribution from the ketyl radicals and ketyl radical anions. Since no extra transition band was needed to fit the transient spectra even at short wavelengths, the presence of an intramolecularly (•S−O)-bonded species was ruled out, although the six-membered ring structure should be thermodynamically possible.

Quantum Yields for Formation of Ketyl Radicals, Ketyl Radical Anions, $(S\therefore S)^+$ Radical Cations, and (•S−O)-Bonded Radicals. The quantum yields for the transients could be obtained in most circumstances. These experiments were done under conditions where the quenching of the triplet of CB was complete (>99%), as calculated from the quenching rate constants in Table 1. Since the intersystem crossing yield of CB is unity,[41] the efficiency of a particular process in the quenching event is equal to the quantum yield of the process. To measure the quantum yields, the relative actinometry method[46,47] was used. For this application, matched optically flat cells containing equal concentrations of CB were used. In the cell used as the actinometer, no quenchers were present, whereas in the sample cell the quencher concentration was typically 20 mM. In the actinometer, the CB triplet's absorbance was monitored at 535 nm immediately after the flash. The quantum yields were calculated according to eq IV

$$\Phi = \Delta A_p \epsilon_T / \Delta A_T \epsilon_p \qquad \text{(IV)}$$

where ΔA_T is the absorption change in the actinometer immediately after the flash due to the CB triplet at 535 nm measured under the condition of no quenching and ΔA_p is the product's absorption change extrapolated to the "end-of-pulse" value under the condition of nearly complete quenching. ϵ_T and ϵ_p are the corresponding molar absorption coefficients. The molar absorption coefficients ϵ_T of the CB triplet and ϵ_p for CBH• and $CB^{\bullet -}$ radicals were normalized[22,43] as mentioned above. The values of ϵ_p for the $(S\therefore S)^+$ dimeric radical cations derived from all the hydroxyalkyl sulfides, and the (•S−O)-bonded radicals of 3-MTP and 3,3′-DHP were taken from Table 2.

Since the absorption spectra of CBH•, $CB^{\bullet -}$, $(S\therefore S)^+$ dimers, and (•S−O)-bonded intermediates overlap, it was necessary to resolve the spectra before the quantum yields could be computed. Time-resolved transient spectra were generated from kinetic traces collected at 37 distinct wavelengths, as described in the preceding section. Spectral resolutions were made at the appropriate points in time. From this procedure, a concentration profile is produced for each of the transients, because each spectral resolution yields one complete set of transient concentrations at a particular time. The primary quantum yields could be then estimated by extrapolating the concentration profiles to zero time. For each quantum yield, five concentrations were determined at uniform time increments over an approximately 1 μs time interval after the laser flash. The concentrations were then extrapolated back to the flash by a least-squares linear fit to the five concentrations giving extrapolated concentrations, c_0. From eq IV, the quantum yields of the transient are then simply

$$\Phi = c_0/c_T \qquad \text{(V)}$$

where c_T is the initial triplet concentration in the actinometer. The resulting quantum yields are shown in Table 3.

This procedure was more elaborate than the previous method[17−19,21] of simply solving eq III for n transients using n wavelengths. The more elaborate technique was used, because it was found that when the (•S−O)-bonded transient was present, the n-wavelength method was very sensitive to the absorbance at 400 nm. To compensate for this sensitivity, the spectral resolution method of determining the transients' concentrations uses the whole spread of wavelengths. For cases not involving (•S−O), both the n-wavelength method and the spectral resolution technique gave almost identical results. The spectral resolution method was used to obtain all reported quantum yields in Table 3.

Supplementary measurements of the quantum yields for all species (CBH•, $CB^{\bullet -}$, $(S\therefore S)^+$, and (•S−O)) were made in D_2O. (For simplicity, CBH• will be used for both the deuteronated and protonated ketyl radical.) Under these conditions the alcohol groups of all the hydroxyalkyl sulfides studied undergo instantaneous H/D exchange with the D_2O solvent (confirmed by ^{1}H-NMR as described in ref 13). All quantum yields measured in D_2O are summarized in Table 3.

Similarities with and Contrasts to Dimethyl Sulfide. Since neighboring groups actively participate in the one-electron photooxidation of organic thioethers,[18,19,21,22,48] we have employed dimethyl sulfide (DMS) as a reference system for the hydroxyalkyl sulfides. Such an approach has two important advantages for this type of mechanistic study. (i) The initial step during one-electron oxidation is expected to be the same

(46) Lutz, H.; Breheret, E.; Lindqvist, L. *J. Phys. Chem.* **1973**, *77*, 1758−1762.

(47) Carmichael, I.; Hug, G. L. *J. Phys. Chem. Ref. Data* **1986**, *15*, 1−250.

(48) Hug, G. L.; Marciniak, B.; Bobrowski, K. *J. Photochem. Photobiol. A* **1996**, *95*, 81−88.

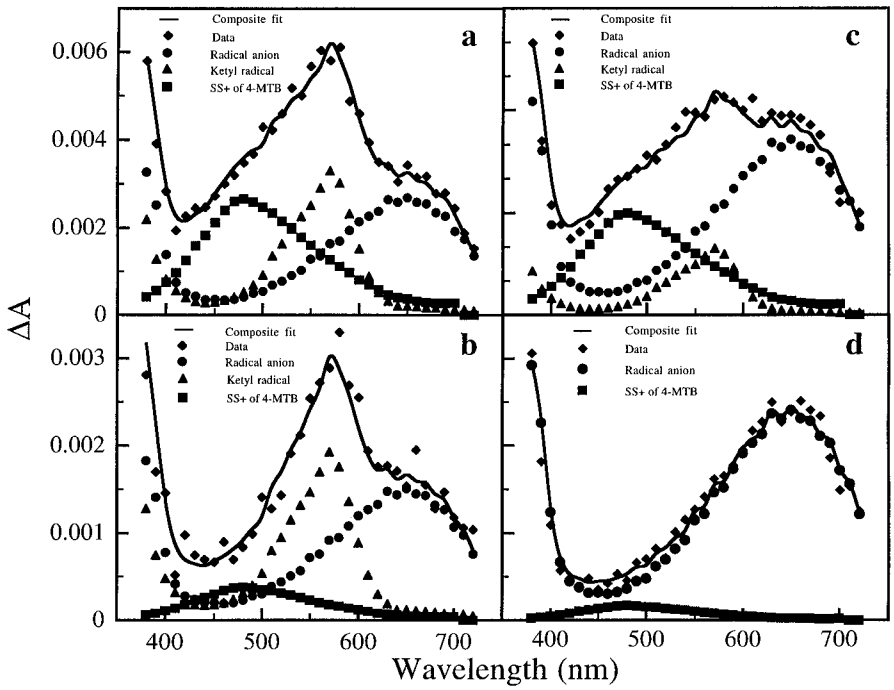

Figure 3. Resolution of the spectral components in the transient absorption spectra following the quenching of CB-triplet by 4-MTB (0.02 M) at pH 6.3 (without buffer) taken (a) 1.6 μs, (b) 53 μs after the flash, and at pH 10.1 (c) 780 ns after the flash and (d) 53 μs after the flash.

Table 3. Quantum Yields of Product Formation in the CB-Sensitized Photooxidation of Sulfur-Containing Alcohols in Neutral (pH 6.7) and Alkaline (pH 10) Solutions[a]

alcohol	solvent	$\Phi_{CBH^{\bullet}+CB^{\bullet-}}$[b,c]	$\Phi_{CBH^{\bullet}}$[c,d]	$\Phi_{CB^{\bullet-}}$[d]	$\Phi_{(S\therefore S)^+}$[d]	$\Phi_{(^{\bullet}S-O)}$[d]
2-MTE	H_2O	0.29 (0.31)	0.17 (0.19)	0.12 (0.12)	0.11 (0.11)	*e*
	D_2O	0.28 (0.31)	0.19 (0.22)	0.09 (0.09)	0.08 (0.09)	*e*
2,2′-DHE	H_2O	0.35 (0.37)	0.29 (0.30)	0.06 (0.07)	0.05 (0.06)	*e*
	D_2O	0.35	0.31	0.04	0.04	*e*
3-MTP	H_2O	0.58 (0.55)	0.35 (0.33)	0.23 (0.22)	0.21 (0.21)	0.32 (0.32)
	D_2O	0.47 (0.51)	0.26 (0.28)	0.21 (0.23)	0.22 (0.26)	0.16 (0.13)
3,3′-DHP	H_2O	0.62	0.46	0.16	0.22	0.50
	D_2O	0.51	0.35	0.16	0.24	0.34
4-MTB	H_2O	0.33	0.20	0.13	0.12	*e*
	D_2O	0.28	0.19	0.09	0.08	*e*

[a] Numbers in parantheses are for alkaline solutions. [b] Sum of $\Phi_{CBH^{\bullet}} + \Phi_{CB^{\bullet-}}$. [c] Deuteronated ketyl radical formed in D_2O. [d] Based on spectral mix (see text). [e] Not observed (see text).

Table 4. Quantum Yields of Product Formation in the CB-Sensitized Photooxidation of Dimethyl Sulfide (DMS) in Neutral and Alkaline Solutions

pH	solvent	$\Phi_{CBH^{\bullet}+CB^{\bullet-}}$[a]	$\Phi_{CBH^{\bullet}}$[b]	$\Phi_{CB^{\bullet-}}$[b]	$\Phi_{(S\therefore S)^+}$[b]
6.7	H_2O	0.29	0.12	0.17	0.20
	D_2O	0.23	0.13	0.10	0.12
9.9	H_2O	0.30	0.11	0.19	0.22
	D_2O	0.25	0.13	0.12	0.15

[a] Sum of $\Phi_{CBH^{\bullet}} + \Phi_{CB^{\bullet-}}$. [b] Based on spectral mix (see text).

in DMS and the hydroxyalkyl sulfides, i.e., formation of the charge-transfer complex, involving a sulfur of the thioether group and an oxygen of the carbonyl group of CB. (ii) DMS lacks other functionalities which could affect reactions within the CT-complex.[17] Thus, any differences in quantum yields of the quenching products observed for the hydroxyalkyl sulfides as compared to DMS can then be ascribed to an involvement of the hydroxyl group(s). With DMS as the CB-triplet quencher, measurements were made of the quantum yields for all the transient species ($CBH^{\bullet}$, $CB^{\bullet-}$, and $(S\therefore S)^+$) in H_2O and D_2O. The values are summarized in Table 4.

Decay Kinetics of $(S\therefore S)^+$. The decay of the $(S\therefore S)^+$-bonded intermediates was followed using the same time-resolved spectral-resolution methods as those used for determining the concentrations of transients for the primary quantum yields (see above). The only difference was that the time scale needed to be expanded to get a reasonable sampling of points for the relatively complex decay curves. For this, about 25 time points were needed. Three different fitting functions were used: single exponential, biexponential, and mixed (parallel first- and second-order decay). The single exponential fits were poor, but there was not much difference in the goodness-of-fit, χ_r^2, between the biexponential and mixed fits. The fast components of the biexponential decays of the $(S\therefore S)^+$ radical cations of 2-MTE are listed in Table 5. The values are tabulated so as to show any variation with pH or deuteration of the solvent. The first-order component of the mixed decays differed in absolute magnitude from the fast components of the biexponential fits,

Table 5. Decay Rate Constants of $(S\therefore S)^+$ Radical Cations of 2-MTE Following the Quenching of CB Triplets

solvent	pH/pD	buffer	k_{fast}[a] (s^{-1})
H_2O	6.82	none	8.7×10^4
D_2O	6.97	none	6.7×10^4
H_2O	8.38	none	5.5×10^4
D_2O	8.55	none	4.8×10^4
H_2O	9.91	none	1.3×10^5
D_2O	10.0	none	1.0×10^5

[a] Fast component from biexponential fit to concentration profiles from spectral resolutions.

Table 6. Quantum Yields Formaldehyde Formation in the CB-Sensitized Photooxidation of Sulfur-Containing Alcohols in Neutral and Alkaline Solution

alcohol	solvent	buffer	pH 6.7	pH 8.0	pH 10
2-MTE	H_2O	none	0.052	0.111	0.096
2-MTE	D_2O	none	0.021	0.019	0.025
2,2′-DHE	H_2O	none	0.074	0.070	0.068
2,2′-DHE	D_2O	none	0.021	0.009	0.015

but the trends in variation with the two solvent parameters (pH and deuteration) were similar.

Formaldehyde Quantum Yields. Quantum yields of formaldehyde ($H_2C{=}O$) formation were measured in the steady-state irradiation of CB solutions (0.5 mM) with 2-MTE and 2,2′-DHE present at a concentration of 6 mM at various pH's. These quantum yields are listed in Table 6.

Discussion

1. Quenching Rate Constants. The rate constants k_q for quenching of the CB triplet state by hydroxyalkyl sulfides (Table 1) are high (approaching one-third of diffusion controlled) and comparable with those for sulfur-containing carboxylic acids,[18] amino acids,[19,20] and methionine-containing peptides.[22] This would put the quenching rate constants at the plateau value of Rehm−Weller plots, corresponding to diffusion-limited reactions. On the other hand, for aliphatic alcohols, which lack a sulfur moiety, the k_q's are 4 orders of magnitude lower[49] than the k_q's obtained for the sulfur-containing alcohols. This supports the idea that the quenching of the CB triplet state by hydroxyalkyl sulfides involves an interaction at the sulfur atom. The mechanism for this triplet quenching process by other sulfur-containing organic compounds was established previously as an electron transfer from the sulfur atom to the triplet species.

2. Transient Spectra. The observed electron-transfer intermediates included $CB^{\bullet-}$, $CBH^{\bullet}$, intermolecularly $(S\therefore S)$-bonded radical cations, and, in the case of 3-MTP and 3,3′-DHP, intramolecularly $(^{\bullet}S\therefore O)$-bonded radicals. 3-MTP and 3,3′-DHP differ from the other alcohols in this work in that they can form conformationally favorable five-membered $(^{\bullet}S-O)$-bonded ring structures. This permits the interaction of an unpaired electron on the sulfur with a nonbonded electron pair on the oxygen atom of the hydroxyl group. The $CB^{\bullet-}$, $CBH^{\bullet}$, and $(S\therefore S)^+$ radical cations of 2-MTE[13] and 2,2′-DHE[35] transient spectra have also been previously reported in the literature.

Resolutions of the transient spectra from flash photolysis demonstrated that formation of the $(S\therefore S)^+$ radical cations of 2-MTE and 2,2′-DHE is not restricted to the low pH region. This is in contrast to the $^{\bullet}OH$-induced oxidation of these hydroxyalkyl sulfides where $(S\therefore S)^+$ radical cations were only observed at pH $\leq$ 2.[13] Data generated from flash photolysis are displayed in Figure 1 and in Table 3 which show that the $(S\therefore S)^+$ radical cations of 2-MTE and 2,2′-DHE are formed even in the pH range 6.9−10. The explanation for this contrasting behavior lies in that the CB-sensitized oxidation of 2-MTE and 2,2′-DHE leads initially to the sulfur-centered radical cations $>S^{\bullet+}$

$$^3CB^* + R_2S \rightarrow CB^{\bullet-} + R_2S^{\bullet+} \quad (\mathbf{1}) \qquad (11)$$

which subsequently associate with an unoxidized hydroxyalkyl sulfide, yielding the $(S\therefore S)^+$ radical cations.

$$R_2S^{\bullet+} + SR_2 \rightleftarrows [R_2S\therefore SR_2]^+ \quad (\mathbf{2}) \qquad (12)$$

(49) Scaiano, J. C. *J. Photochem.* **1973**, *2*, 81−118.

In contrast, pulse-radiolytically generated $^{\bullet}OH$-adducts of 2-MTE and 2,2′-DHE do not yield measurable yields of $(S\therefore S)^+$ radical cations in neutral and alkaline solutions.[13] These $^{\bullet}OH$-adducts, thus, appear to react by a different mechanism which confirms our previous assessment that they may decompose by the elimination of water. The water could be formed through a rapid intramolecular proton or hydrogen transfer from the adjacent hydroxyl group. The latter mechanism leads to the formation of (alkylthio)ethoxy radicals which subsequently undergo α,β-fragmentation into formaldehyde and an α-(alkylthio)alkyl radical (see reaction 5). This will be discussed further below.

3. Mechanism of Formation of Transients: Isotope Effects. In general, the formation of the three-electron bonded dimers $[R_2S\therefore SR_2]^+$ in triplet-quenching events involves reactions 11 and 12, followed by association of the generated radical cation $R_2S^{\bullet+}$ with a second nonoxidized sulfur (reaction 12). However, since we observe solvent isotope effects on the yields of radical cations that vary with the nature of the thioether, it appears that the mechanism of reaction is more complex. In the following, different possible mechanisms will be considered for each of the sulfides investigated. The isotope effects will be rationalized qualitatively rather than quantitatively since geometries and charge distributions in transition state(s) and/or intermediates are at present largely unknown.

In the following discussion, the "product" species will usually refer to the ion-pair (IP) state. The total secondary kinetic solvent isotope effect can be written as[50,51]

$$\frac{k_H}{k_D} = \frac{\prod_i \phi_i^R}{\prod_j \phi_j^{IP}} \qquad (VI)$$

where ϕ^R and ϕ^{IP} represent the fractionation factors of various hydrogenic sites in the reactant form and in the ion pair, respectively. The isotopic fractionation factor of a particular hydrogenic site in a chemical species is defined as the ratio of that site's preference for deuterium over protium relative to the similar preference for a single hydrogenic site in a solvent molecule. The isotopic fractionation factor of a hydrogenic site attached to a neutral oxygen is defined as one. Some other common examples are $\phi = 0.69$ for hydrogenic sites attached to a positively-charged oxygen and $\phi = 0.5$ for hydrogenic sites attached to a negatively-charged oxygen.[50]

Dimethyl Sulfide (DMS). For better comparison between the schemes, all reactions in the schemes have been assigned numbers which directly relate them to the schemes (i.e., 1.1, 1.2 for Scheme 1; 2.1, 2.2 for Scheme 2; etc.). The first step in the one-electron oxidation process of DMS represents the formation of charge-transfer complex **3a**, shown in reaction 1.1 in Scheme 1. In the course of reaction 1.1 two neutral reactants (neglecting the 4-carboxy group of CB which does not participate in the reaction) associate to yield the dipolar charge-transfer complex **3a**. According to the mechanism previously proposed,[17] complex **3a** either suffers back electron transfer to yield ground state CB and DMS (reaction 1.2, Scheme 1), undergoes hydrogen transfer (reaction 1.3, Scheme 1), or diffuses apart to yield product radical ions ($>S^{\bullet+}$ and $CB^{\bullet-}$).

The yield of the solvated product $[(H_3C)_2S\therefore S(CH_3)_2]^+$ (**2a**) shows a product solvent isotope effect of $[\mathbf{2a}]_{H_2O}/[\mathbf{2a}]_{D_2O} = 1.7$

(50) Schowen, R. L. In *Progress in Physical Organic Chemistry*; Streitwieser, A., Jr.; Taft, R. W., Eds.; Wiley: New York, 1972; Vol. 9, pp 275−332.

(51) Schowen, K. B. J. In *Transition States of Biological Processes*; Gandour, R. D.; Schowen, R. L., Eds.; Plenum Press: 1978; pp 225−283.

Scheme 1

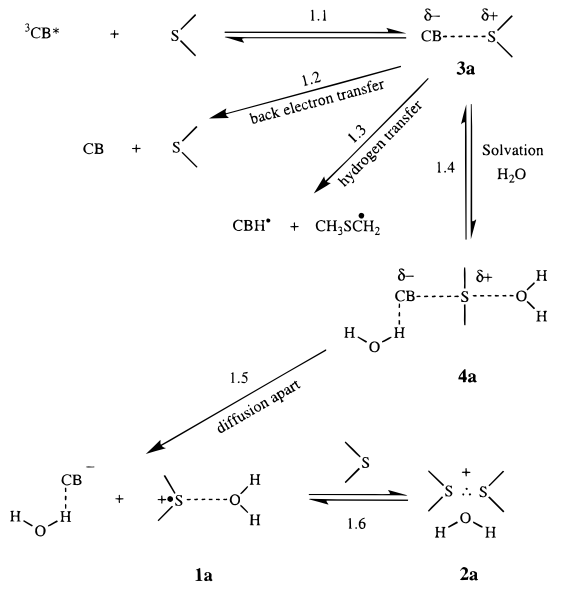

Scheme 2

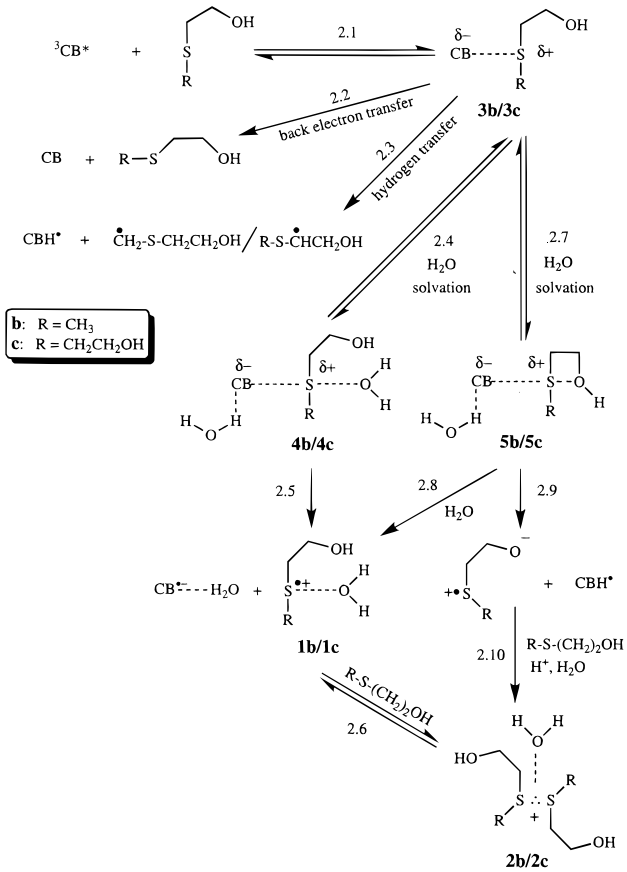

at pH 6.7 (calculated from Table 4). This is a rather surprising observation since products and reactants in the reaction leading to radical ions do not have exchangeable protons. This observation can be rationalized by postulating the formation of the solvated ion pair (**4a**) (reaction 1.4, Scheme 1). The degree of solvation will determine the probability of a successful separation of the ion pair **4a** into solvated product ions $>S^{\bullet+}$ (**1a**) and $CB^{\bullet-}$ (reaction 1.5, Scheme 1) which is in competition to reactions 1.2 and 1.3 of Scheme 1. It is noteworthy that the product solvent isotope effect for $CB^{\bullet-}$ at pH 6.7 was similar to that for the $(S\therefore S)^+$ transient ($[CB^{\bullet-}]_{H_2O}/[CB^{\bullet-}]_{D_2O} = 1.7$, calculated from Table 4). Subsequently, **1a** will associate with a nonoxidized sulfide to yield the dimeric sulfide radical cation **2a** (reaction 1.6, Scheme 1), which is observable through its spectrum with $\lambda_{max} = 465$ nm. Since there is no rate determining proton transfer step associated with reactions 1.4 and 1.5, eq VI[50,51] predicts a normal solvent isotope effect of $k_H/k_D > 1.0$ for the overall electron-transfer process. Such a prediction is based on the competition of reactions 1.4 and 1.5 with reactions 1.2 and 1.3 where we do not expect any solvent isotope effect on the individual reactions 1.2 and 1.3. This is confirmed for reaction 1.3 by the lack of a solvent isotope effect on the ketyl radical yield ($CBH^{\bullet}$) (Table 4).

As a result of the solvation, the fractionation factors of the hydrogen atoms of the solvating water molecules will change from $\phi^R = 1.0$ to $\phi^{IP} < 1.0$. It is difficult to predict the magnitude of the expected solvent isotope effect since we do not know (i) the partial charges $\delta-$ on CB and $\delta+$ on the sulfide in the solvated ion pair **4a**, (ii) the partial charges on the solvating water molecules, and (iii) the fractionation factor of the proton shared between water and the negatively charged oxygen atom of the developing ketyl radical anion, $CB^{\delta-}$, in the solvated ion pair **4a**.

2-(Methylthio)ethanol (2-MTE) and 2,2′-Dihydroxydiethyl Sulfide (2,2′-DHE). The formation of the radical cation complexes of 2-MTE, **2b**, and 2,2′-DHE, **2c**, shows product isotope effects of $[\mathbf{2b}]_{H_2O}/[\mathbf{2b}]_{D_2O} = 1.4$ and $[\mathbf{2c}]_{H_2O}/[\mathbf{2c}]_{D_2O} =$ $= 1.25$, respectively (calculated from Table 3). They are smaller than the corresponding product isotope effect of the $(S\therefore S)^+$ yield in DMS of 1.7. This can be rationalized on the basis of a mechanism displayed in Scheme 2.

The first steps of the reaction of $^3CB^*$ with the hydroxyalkyl sulfides 2-MTE and 2,2′-DHE are exactly analogous to those involving DMS and yield the charge-transfer complexes **3b**/**3c** (reaction 2.1, Scheme 2). Subsequently, also in analogy to DMS, solvation of the charge-transfer complex **3b**/**3c** (reaction 2.4, Scheme 2) competes with back electron transfer (reaction 2.2) and hydrogen transfer (reaction 2.3). However, there is an additional channel open to the charge-transfer complexes **3b**/**3c** in comparison to **3a** in the DMS case. For **3b**/**3c**, instead of solvating through the interaction of an oxygen from a solvent molecule, the sulfur atom in the developing radical cation may also interact with the oxygen of the terminal hydroxy group(s) (**5b**/**5c**) of 2-MTE or 2,2′-DHE, (reaction 2.7, Scheme 2). Separated radical ions can escape (reaction 2.8, Scheme 2) from **5b**/**5c** to yield **1b**/**1c**. Species **1b**/**1c** may also directly result from the separation of the solvated ion pair **4b**/**4c** by reaction 2.5. An alternate fate of **5b**/**5c** is a proton-transfer step within the complex **5b**/**5c** and escape of the resulting radicals by reaction 2.9 in Scheme 2. This proton transfer and the escape of $CBH^{\bullet}$ may be particularly important in the pH range below the $pK_a = 8.2$[41] of $CBH^{\bullet}$.

The key to understanding the differences between the solvent isotope effects seen in the two thioethanols and DMS lies in the competing reaction paths 2.4 vs 2.7 in Scheme 2. A comparison of the structures of **5b**/**5c** with those of **4a**, **4b**, and **4c** reveals that **5b**/**5c** has one less proton on the oxygen directly associated with the sulfur. Since the fractionation factor for a proton is $\phi_{H^+} = 0.69$, the denominator $\prod_j \phi_j^{IP}$ in eq VI should be larger for the formation (reaction 2.7, Scheme 2) of **5b**/**5c** (one proton) than for the formation (reaction 2.4, Scheme 2) of **4b**/**4c** (two protons). With a larger denominator in eq VI for reaction path 2.7, Scheme 2, its solvent isotope effect should be smaller than that of reaction path 2.4. Therefore, to the extent that the reaction channels 2.4 and 2.7 are effectively competing, the overall solvent isotope effect should be smaller than going exclusively through reaction path 2.4 which is the analog to

the only path available to DMS in reaction 1.4, Scheme 1. In a similar line of argument, the extra hydroxyethyl group in 2,2′-DHE is likely to enhance the competition of reaction 2.7 vs reaction 2.4 in comparison to 2-MTE and, thus, lower the overall solvent isotope effect of 2,2′-DHE compared to 2-MTE. Both of these expectations are verified in the experiments. These conclusions are based on the assumption that the positive partial charge on the sulfur and the oxygen atoms are similar for **4a**, **4b**/**4c**, and **5b**/**5c**.

3-(Methylthio)propanol (3-MTP) and 3,3′-Dihydroxydipropyl Sulfide (3,3′-DHP). For 3-MTP and 3,3′-DHP, there is no solvent isotope effect, within experimental error, on the yields of sulfide radical cations **2d**/**2e**. However, there is a significant normal solvent isotope effect on the yields of a sulfur−oxygen bonded intermediate **7d**/**7e** (Scheme 3). The solvent isotope effects in the product yields are $[\mathbf{7d}]_{H_2O}/[\mathbf{7d}]_{D_2O} = 2.0$ for 3-MTP and $[\mathbf{7e}]_{H_2O}/[\mathbf{7e}]_{D_2O} = 1.5$ for 3,3′-DHP (calculated from Table 3). In principle, these isotope effects can be rationalized by a mechanism displayed in Scheme 3. It was proposed to be as closely analogous as possible to the mechanism presented for the ethanol derivatives in Scheme 2.

However, certain critical differences apply which are of significance in understanding solvent isotope effects on the quantum yields of transients. In general, formation of five-membered sulfur−oxygen (and sulfur−nitrogen) bonded intermediates such as **6d**/**6e** and **7d**/**7e** is fast, leading to an intramolecular bond formation involving the developing sulfide-radical-cation moiety. In addition, these five-membered sulfide−oxygen bonded intermediates are relatively stable for the propanol derivatives, in contrast to the four-membered rings in the ethanol derivatives.[13] It is of particular significance to this discussion that sulfur−oxygen transients involving hydroxyl moieties can deprotonate[4] and that the acidity of the hydroxyl group is greatly enhanced over the hydroxyl group in the unoxidized hydroxyalkyl sulfide. The sulfur−oxygen bonded intermediates derived from 3-MTP (**6d**, **7d**) and 3,3′-DHP (**6e**, **7e**) exist in the acid−base equilibrium (reaction 3.13, Scheme 3) with $pK_a \approx 4.7$.[52]

In order to understand the solvent isotope effects, it is important to note from Table 3 that $\Phi_{CBH\bullet} \approx \Phi_{(\bullet S-O)}$ and that $\Phi_{CB\bullet-} \approx \Phi_{S\therefore S^+}$ for the propanol derivatives. From this it is reasonable to conclude that the formation processes of $CBH^\bullet$ and ($^\bullet S-O$) intermediates are coupled and that the formation of $(S\therefore S)^+$ intermediates is the main pathway of $>S^{\bullet+}$ radical cation decay. For Scheme 3 to accommodate these observations, certain conclusions can be drawn about the rate constants in Scheme 3: (a) the equilibrium 3.12 between **6d**/**6e** and **1d**/**1e** would have to be very slow, (b) reaction 3.11 would also be slow, and (c) hydrogen-transfer reaction 3.3 from **3d**/**3e** would be slow. Such an alignment of equilibria and rate constants would account for $\Phi_{CBH\bullet} \approx \Phi_{(\bullet S-O)}$ and $\Phi_{CB\bullet-} \approx \Phi_{S\therefore S^+}$ in the propanol derivatives. Deviations from the equalities between these quantum yields might be accounted for by some or all of the rate processes in (a), (b), and (c) being nonzero, see below.

With such restrictions on the rate processes in Scheme 3, it can be seen that $CB^{\bullet-}$ and $(S\therefore S)^+$ are formed mainly from the sequence of reactions 3.4/3.5/3.6; whereas $CBH^\bullet$ and ($^\bullet S-O$) are mainly formed in the sequence of reactions 3.7/3.9/3.14. The normal solvent isotope effect on the formation of $CBH^\bullet$ and ($^\bullet S-O$) would come through equilibrium 3.7 and/or a rate-determining proton transfer in reaction 3.9, see calculation below. On the other hand, the expected normal solvent isotope effect on the formation of $(S\therefore S)^+$ and $CB^{\bullet-}$ was not observed.

(52) Wisniowski, P.; Hug, G. L.; Bobrowski, K. Manuscript in preparation.

Scheme 3

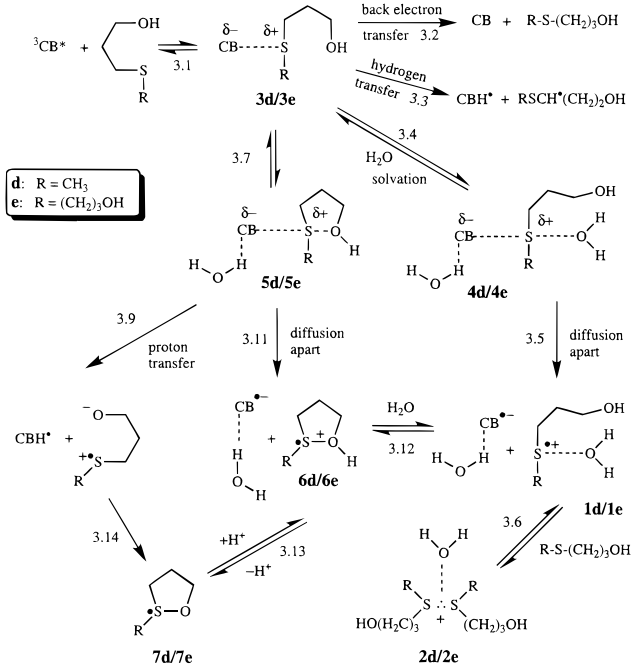

This could be due to the competition with reaction 3.9 having a large normal solvent isotope effect. The apparent small inverse solvent isotope effect could arise if reaction 3.9 dominates for the H_2O reaction, but for the D_2O reactions, reaction 3.9 is supressed relatively more than 3.4 or 3.11, possibly making them competitive with 3.9.

It is of note that the solvent isotope effects for the propanol derivatives are generally larger than for the ethanol derivatives, i.e., compare 1.4 for 2-MTE vs 2.0 for 3-MTP and 1.25 for 2,2′-DHE vs 1.5 for 3,3′-DHP. If deprotonation would already occur to a significant extent within the solvated ion pair **5d**/**5e**, we would expect larger normal isotope effects due to the fact that the resulting proton H_3O^+ would appear in the denominator of eq VI as $(\phi_{H^+})^3$ in contrast to $(\phi_{H^+})^2$ for DMS (two water protons in **4a**) and (ϕ_{H^+}) for the ethanol derivatives (one proton of the terminal hydroxyl group in **5b**/**5c**). An alternative explanation for the larger isotope effects in the propanol derivatives could be related to contributions from primary isotope effects due to a rate-determining proton transfer (within structures **5d**/**5e**) in the course of reactions 3.9 and 3.14 of Scheme 3 which directly lead to **7d**/**7e** and formation of ketyl radicals $CBH^\bullet$. This path would likely be enhanced over the analogous path 2.9 of Scheme 2, because the fast formation and stability of **5d**/**5e** of the thiopropanols in comparison to **5b**/**5c** of the thioethanols enables proton transfer within the ion pairs.

4-(Methylthio)butanol. In general, the considerations for 2-MTE and 2,2′-DHE will also apply to 4-(methylthio)butanol which shows a similar solvent isotope effect on the formation of sulfide radical cations as 2-MTE.

4. Quantum Yields of Transients. Although the initial step in the mechanisms (Schemes 2 and 3) is the same for all the hydroxyalkyl sulfides, the primary quantum yields of the various intermediates differ significantly among the hydroxyalkyl sulfides. For 2-MTE, 2,2′-DHE, and 4-MTB, the total quantum yields for ketyl radical ($CBH^\bullet$) and ketyl radical anion ($CB^{\bullet-}$) formation are roughly half the analogous yields for 3-MTP and 3,3′-DHP (Table 3). According to the mechanisms in Schemes 2 and 3, these quantum yields represent the combined yields of two processes, namely the diffusion apart of the charge-transfer

complex (radical ion escape) and the intramolecular proton transfer within the complex. This means that the quantum yield for back electron transfer would be about 60−70% for 2-MTE, 2,2′-DHE, and 4-MTB and 30−35% for 3-MTP and 3,3′-DHP. The quantum yields indicate that, contrary to quenching events of sulfur-containing amino acids[19−21] and carboxylic acids,[18] back electron transfer is an efficient process in quenching events involving hydroxyalkyl sulfides (particularly for 2-MTE, 2,2′-DHE, and 4-MTB). The efficiency of quenching by 2-MTE, 2,2′-DHE, and 4-MTB is comparable to the analogous quenching by unsubstituted alkyl sulfides.[17]

The individual contributions to the yield of primary photoproducts can be separately characterized as being due in part to the escape of radical ions from the charge-transfer complex and to a somewhat greater extent to a proton-transfer reaction within the charge-transfer complex (see the values of $\Phi_{CBH^\bullet}$ in Table 3). The quantum yields for escaping radical ions vary from about 10% for 2-MTE, 2,2′-DHE, and 4-MTB to about 25% for 3-MTP and 3,3′-DHP (see the values of $\Phi_{CB^{\bullet-}}$ and $\Phi_{S\therefore S^+}$ in Table 3). There are significantly higher values of $\Phi_{CBH^\bullet}$ for 3-MTP and 3,3′-DHP compared to the other sulfur-containing alcohols. These higher yields can be explained by the ability of 3-MTP and 3,3′-DHP to form intramolecularly (•S−O)-bonded species. From Table 3, it can be seen that the expected equality $\Phi_{CB^{\bullet-}} + \Phi_{CBH^\bullet} = \Phi_{S\therefore S^+} + \Phi_{\bullet S-O}$ does not quite hold for 3,3′-DHP. This may be due to an error in the smaller than usual molar extinction coefficient of 7300 M^{-1} cm^{-1} for the $(S\therefore S)^+$ species of 3,3′-DHP.

5. Mechanism of Carbon-Carbon Bond Fragmentation for Radical Cations of 2-MTE and 2,2′-DHE. There are several key features that are important to consider for a discussion of the mechanism of carbon−carbon bond fragmentations. (i) The initial yields of **2b**, the $(S\therefore S)^+$ radical cations of 2-MTE, are twice as high as the initial yields of **2c**, the $(S\therefore S)^+$ radical cations of 2,2′-DHE (Table 3). (ii) There are small normal solvent isotope effects on the order of $k_H/k_D \approx 1.3$ on k_{fast} (Table 5). (iii) A computation of various ratios, Ω, of formaldehyde-to-$(S\therefore S)^+$ quantum yields

$$\Omega = \Phi_{H_2CO}/\Phi_{(S\therefore S)^+} \qquad \text{(VII)}$$

for 2-MTE from Tables 3 and 6 give the following: $\Omega_{H_2O}^{neutral} = 0.47$, $\Omega_{D_2O}^{neutral} = 0.25$, $\Omega_{H_2O}^{pH10} = 0.87$, and $\Omega_{D_2O}^{pD10} = 0.28$. For 2,2′-DHE, $\Omega_{H_2O}^{neutral} = 1.5$, $\Omega_{D_2O}^{neutral} = 0.53$, and $\Omega_{H_2O}^{pH10} = 1.1$. The observation that the quantum yields of formaldehyde slightly exceed the initial quantum yields of $(S\therefore S)^+$ for 2,2′-DHE requires some discussion (vide infra). (iv) From Table 6, it can be seen that there is an increasing solvent isotope effect on the formation of formaldehyde with increasing pH. For 2-MTE, $[H_2CO]_{H_2O}/[H_2CO]_{D_2O} = 2.5$ at pH 6.7 and $[H_2CO]_{H_2O}/[H_2CO]_{D_2O} = 3.8$ at pH 10. Similarly for 2,2′-DHE, $[H_2CO]_{H_2O}/[H_2CO]_{D_2O} = 3.5$ at pH 6.7 and $[H_2CO]_{H_2O}/[H_2CO]_{D_2O} = 4.5$ at pH 10.

These observations can be partially rationalized by the mechanisms in Schemes 2 and 4. Increasing yields of formaldehyde can be expected with increasing pH based on an increasingly favorable competition of hydroxide ion attack (for reactions 4.16 and 4.18, Scheme 4) with reverse electron transfer (reaction 4.15, Scheme 4) which does not lead to formaldehyde. At any given pH, formaldehyde will be produced either via reaction sequence 4.16/4.17 or 4.18/4.19. By analogy to the results of Baciocchi et al.[15] and Lucia et al.,[14] reaction 4.18 is expected to have a normal primary solvent isotope effect between 1.2 and 2.0. Reaction 4.16 should exhibit an inverse secondary solvent isotope effect (no rate-determining proton

Scheme 4

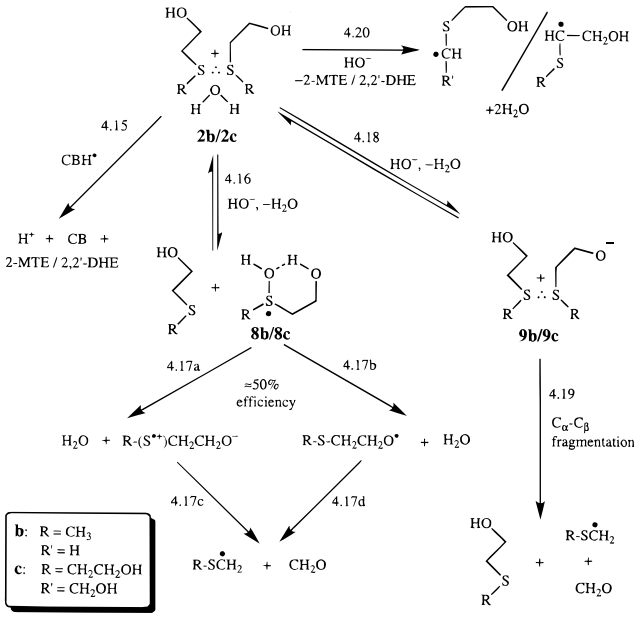

transfer) because from the analogous equation to eq VI[50]

$$K_H/K_D = \phi(HO^-)\phi(H_2O^{\delta+})^{2\delta+}/\phi(\mathbf{8b}/\mathbf{8c}) = (0.5)(0.69)^{2\delta+}/1 < 1 \qquad \text{(VIII)}$$

where $\delta+$ is the positive charge shared by the oxygen in structure **2b**/**2c**. In addition, reaction 4.17 has an experimentally determined solvent isotope effect of unity.[13] If reaction sequence 4.18/4.19 would yield formaldehyde with higher efficiency than reaction sequence 4.16/4.17, a change of the solvent from H_2O to D_2O would cause a normal solvent isotope effect on the formaldehyde yields. However, a more likely contribution to the normal solvent isotope effect arises from the fact that in D_2O, due to the less efficient reaction 4.18 (includes a primary kinetic isotope effect), deprotonation of **2b**/**2c**'s C_α−H bond (which does not exchange protons with the solvent) may excel (reaction 4.20, Scheme 4). This process does not lead to formaldehyde.

At neutral pH, the base-catalyzed reactions 4.16 and 4.18 would have to proceed with water as the base. At pH < $pK_a(CBH^\bullet) = 8.2$ the developing $CB^{\bullet-}$ within the ion pair **5b**/**5c** (Scheme 2) could theoretically act as a base to accept protons from the terminal hydroxyl group of 2-MTE and 2,2′-DHE leading to $CBH^\bullet$ and the monomeric radical cation $^-OCH_2$-$CH_2S^{\bullet+}$-R by reaction 2.9 of Scheme 2. This zwitterion is susceptible to $C_\alpha-C_\beta$ fragmentation analogous to reaction 4.19 for the dimerized radical zwitterion. These considerations, along with the arguments in the preceding paragraph for the high pH range, can explain the normal solvent isotope effect on formaldehyde formation.

However, it should be noted from Scheme 4 that it is estimated that **8b**/**8c** forms formaldehyde in only 50% yield. This is based on gamma radiolysis yields of formaldehyde compared to •OH yields (or >•S−OH) in aqueous solutions of 2-MTE at pH 6.[13] If the unknown reaction channel of **8b**/**8c** that does not yield formaldehyde is more efficient at pH 10, then the inverse solvent isotope effect would be less competitive, and the normal solvent effect could increase with pH as observed. Another possible explanation for this phenomenon is that the base-catalyzed reaction sequence 4.18/4.19 is more efficient at high pH than the reaction 2.9 is at neutral pH.

The quantum yields of formaldehyde can in some cases slightly exceed the initial quantum yields of $(S\therefore S)^+$ as in the

case **2c** from 2,2′-DHE. These observations warrant some discussion. The higher frequency of $C_\alpha-C_\beta$ bond breakage for 2,2′-DHE produces larger quantities of α-(alkylthio)methyl radicals. Disproportionation of the latter leads to additional formaldehyde via reactions 13 and 14.

$$2^{\bullet}CH_2SR \rightarrow {}^{-}CH_2SR + {}^{+}CH_2SR \quad (13)$$

$${}^{+}CH_2SR + H_2O \rightarrow H^{+} + CH_2O + RSH \quad (14)$$

Similar reactions also operate for 2-MTE. However, since the total formaldehyde yields are lower than the initial yields of **2b**, we cannot assess how much processes analogous to reactions 13 and 14 contribute to the formaldehyde yields in the 2-MTE system.

6. Proton Transfer vs Hydrogen Transfer in the •OH Radical-Induced Oxidation Mechanism of 2-MTE and 2,2′-DHE. We are now left with the question whether the hydroxyl-radical-induced fragmentation of 2-MTE and 2,2′-DHE proceeds via proton transfer and sulfide radical cations (reaction 4.17a, Scheme 4) or via hydrogen transfer (reaction 4.17b, Scheme 4), as originally proposed.[13] During the hydroxyl-radical-induced fragmentation, less formaldehyde yields were observed for 2,2′-DHE than for 2-MTE at pH 6.[13] This is in contrast to the one-electron oxidation-induced fragmentation at pH 6.7 in this work. This feature alone may render some support for the originally proposed hydrogen-transfer mechanism.

From the previous discussion it can be seen that both proton transfer and hydrogen transfer appear to operate in the mechanisms of formaldehyde formation in the radiolytic and photolytic oxidation of the thioethanols. Which of the two processes dominate depends on the nature of the oxidant, and, in particular, it depends on the reactive intermediates involved in the oxidation process. In pulse radiolysis experiments using •OH radicals, hydroxysulfuranyl radicals are formed, and both hydrogen-transfer and proton-transfer mechanisms can occur. In contrast in the CB-photosensitized oxidation of 2-MTE and 2,2′-DHE at neutral pH, solvated ion pairs **5b**/**5c** can be formed which can undergo transformation either to $CBH^{\bullet}$ and $RS^{\bullet+}CH_2CH_2O^{-}$ or **1b**/**1c** and $CB^{\bullet-}$ (Scheme 2). Since **1b**/**1c** does not undergo instantaneous fragmentation, it is possible to observe **2b**/**2c** in CB-photosensitized oxidation at all pH values and in pulse radiolysis experiments at pH 1. The **1b**/**1c** cannot be generated by pulse radiolysis at neutral solution using the •OH radical as an oxidant, which accounts for the lack of **2b**/**2c** in pulse radiolysis experiments at neutral pH.

How can we describe the potential hydrogen transfer process mechanistically? In its reaction with 2-MTE, the hydroxyl radical will be initially trapped by the sulfur atom but probably exists in equilibrium 15.

$$CH_3SCH_2CH_2OH + {}^{\bullet}OH \rightleftarrows CH_3S^{\bullet}(OH)CH_2CH_2OH \quad (15)$$

If a cyclic structure such as **8b** were to exist, homolytic dissociation (the reverse of the oxidation reaction) of the hydroxysulfuranyl radical would yield a hydroxyl radical in the immediate vicinity of the terminal hydroxyl group. In general, hydrogen abstraction by •OH from hydroxyl groups is possible,[53] and its probable occurrence would be enhanced by the spatial closeness of the reactants in these circumstances.

Acknowledgment. The work described herein was supported by the Office of Basic Energy Sciences of the U.S. Department of Energy (K.B., G.L.H., and B.M.), the Committee of Scientific Research, Poland (Grant No. 2 P303 049 06) (B. M. and K. B.), a Self-Fellowship (B. M.), and the Association for International Cancer Research (Ch.S.). The authors thank Professor K.-D. Asmus and Dr. I. Carmichael for instructive conversations. This paper is Document No. NDRL-3988 from the Notre Dame Radiation Laboratory.

JA970683R

(53) Asmus, K.-D.; Möckel, H.; Henglein, A. *J. Phys. Chem.* **1973**, *77*, 1218−1221.